1-Benzoylazoles: An experimental (NMR and crystallography) and theoretical study

ARTICLE *in* JOURNAL OF MOLECULAR STRUCTURE · MARCH 2002

Impact Factor: 1.6 · DOI: 10.1016/S0022-2860(01)00759-1

ELSEVIER

Journal of Molecular Structure 605 (2002) 199–212

Journal of
MOLECULAR
STRUCTURE

www.elsevier.com/locate/molstruc

1-Benzoylazoles: an experimental (NMR and crystallography) and theoretical study

R.M. Claramunt[a], P. Cornago[a], D. Sanz[a], M.D. Santa-María[a], C. Foces-Foces[b], I. Alkorta[c], J. Elguero[c,*]

[a]*Departamento de Química Orgánica y Biología, Facultad de Ciencias, UNED, Senda del Rey 9, 28040 Madrid, Spain*
[b]*Departamento de Cristalografía, Instituto de Química-Física Rocasolano, CSIC, Serrano 119, 28006 Madrid, Spain*
[c]*Instituto de Química Médica, Centro de Química Orgánica 'Manuel Lora Tamayo', CSIC, Juan de la Cierva 3, 28006 Madrid, Spain*

Received 30 April 2001; revised 12 June 2001; accepted 12 June 2001

Abstract

Five *N*-benzoylazoles (imidazole, pyrazole, indole, benzimidazole and carbazole) have been prepared following modified literature procedures. Their NMR spectra in solution (^{1}H, ^{13}C and ^{15}N) have been measured. The crystal structures of 1-benzoylindole and 9-benzoylcarbazole have been determined by X-ray crystallography and the corresponding ^{13}C NMR spectra in the solid state have been measured by the CPMAS technique. Whereas 1-benzoylindole presents a standard behaviour, 9-benzoylcarbazole shows an unexpected ^{13}C CPMAS spectrum with additional splittings. In order to understand this fact, the ^{1}H and ^{13}C NMR spectra in dimethylether at −143°C (130 K) have been recorded and ab initio calculations (RHF/6-311G**) carried out. The corresponding absolute shieldings (GIAO/ RHF/6-311G**) together with the X-ray structure and the ^{13}C chemical shifts at low temperature have been used to discuss the CPMAS spectrum. We propose that the supplementary splittings of this spectrum are due to its conglomerate structure.

Keywords: Azolides; NMR; CPMAS NMR; Rotational barriers; X-ray crystallography; ab initio calculations

1. Introduction

We have been studying the physico–chemical properties of azolides for a long time. These studies concern mainly their NMR properties, generally in solution [1–5], but also in the solid state [6], and their behaviour in mass spectrometry [7,8]. Recently, we have written a review [9] and a subsequent paper on ab initio calculations of their *N*—CHO, *N*—$COCH_3$, *N*—$COCF_3$ and *N*—CO_2CH_3 derivatives [10].

The present work reports the results we have obtained for five *N*-benzoylazoles: namely, 1-benzoylimidazole **1**, 1-benzoylpyrazole **2**, 1-benzoylindole **3**, 1-benzoylbenzimidazole **4** and 9-benzoylcarbazole **5**.

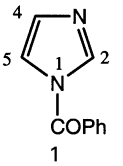

1

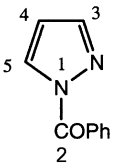

2

* Corresponding author. Tel.: +34-91411-0874; fax: +34-91564-4853.
E-mail address: iqmbe17@iqm.csic.es (J. Elguero).

0022-2860/02/$ - see front matter
PII: S0022-2860(01)00759-1

Table 1
Selected geometrical parameters (Å,°). Cent(A, B, C or D) stands for the centroid of the corresponding A, B, C or D rings as shown in Fig. 1

Compound **3**		Compound **5**		
N1—C10	1.394(2)	N1—C14	1.400(7)	
C10—O17	1.211(2)	C14—O15	1.212(7)	
N1—C10—O17	120.8(1)	N1—C14—O15	119.3(5)	
C9—N1—C10	125.9(1)	C2—N1—C14	124.6(5)	
C2—N1—C14	126.0(1)	C13—N1—C14	127.6(4)	
C2—N1—C9	107.1(1)	C2—N1—C13	107.7(4)	
C9—N1—C10—O17	−6.1(2)	C2—N1—C14—O15	−23.5(9)	
N1—C10—C11—C12	−45.0(2)	N1—C14—C16—C17	−45.7(8)	
A ∧ B	1.3(1)	A ∧ B	1.3(2)	
		B ∧ C	5.2(2)	
Hydrogen interactions:	D—H	H···A	D···A	D—H···A
Compound: **3**				
C8—H8···O17	0.97(2)	2.42(2)	2.938(2)	113(2)
C16—H16···Cent(B)(1 − *x*, − y,1 − *z*)	1.02(2)	2.72(2)	3.520(2)	135(2)
C13—H13···Cent(A)(1 − *x*,1 − *y*,2 − *z*)	0.98(3)	2.79(2)	3.600(2)	140(2)
C3—H3···Cent(D)(1 − *x*, − y,2 − *z*)	1.01(3)	2.85(3)	3.665(2)	138(2)
Compound: **5**				
C3—H3···O15	0.96(7)	2.26(7)	2.890(9)	122(5)
C4—H4···O15(1/2 − *x*,1 − *y*,1/2 + *z*)	0.99(6)	2.66(6)	3.393(7)	131(5)
C19—H19···Cent(C)(1/2 − *x*, − *y*, − 1/2 + *z*)	1.01(7)	2.87(7)	3.867(8)	167(6)

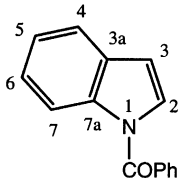

3

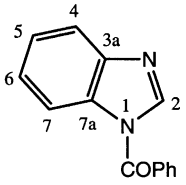

4

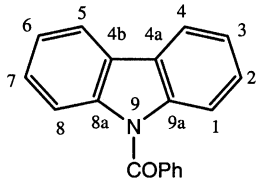

5

2. Results and discussion

2.1. Chemistry

The five compounds are known compounds, one being liquid at room temperature: **1**, m.p. 20–21°C [11], the other solids, in which cases the melting points coincide with those of the literature: **2**, m.p. 46°C [12], **3**, m.p. 69°C [13], **4**, m.p. 91–92°C [14,15], **5**, m.p. 98°C [16].

2.2. X-ray crystallography

The main geometrical intra and intermolecular parameters for compounds **3** and **5** are reported in Table 1. The molecular structure of **3** presents similar features regarding the 'amide' fragment to those described for other 1-COR-indole derivatives [9,17], that is, N—C, C=O distances, N—C=O angle and, as in almost all structures, the C=O group pointing towards the benzene ring [Fig. 1(a)]. Greater discrepancies (C=O distance and N—C=O angle) between **5** [Fig. 1(c)] and the only 9-COR-carbazole derivative previously reported (14-acetyl-di-indolo[2,3-*a*:2′,3′-*c*]carbazole; CSD refcode: INDCBZ10) [18], are observed. They are probably due to the tricyclic fused ring system and to the low precision achieved in INDCBZ10 (R = 10.4%). In **3** and **5**, the indole and the carbazole moieties (*N*-substituted with benzoyl groups) show small but significant distortions from planarity. The angles between the least-squares planes

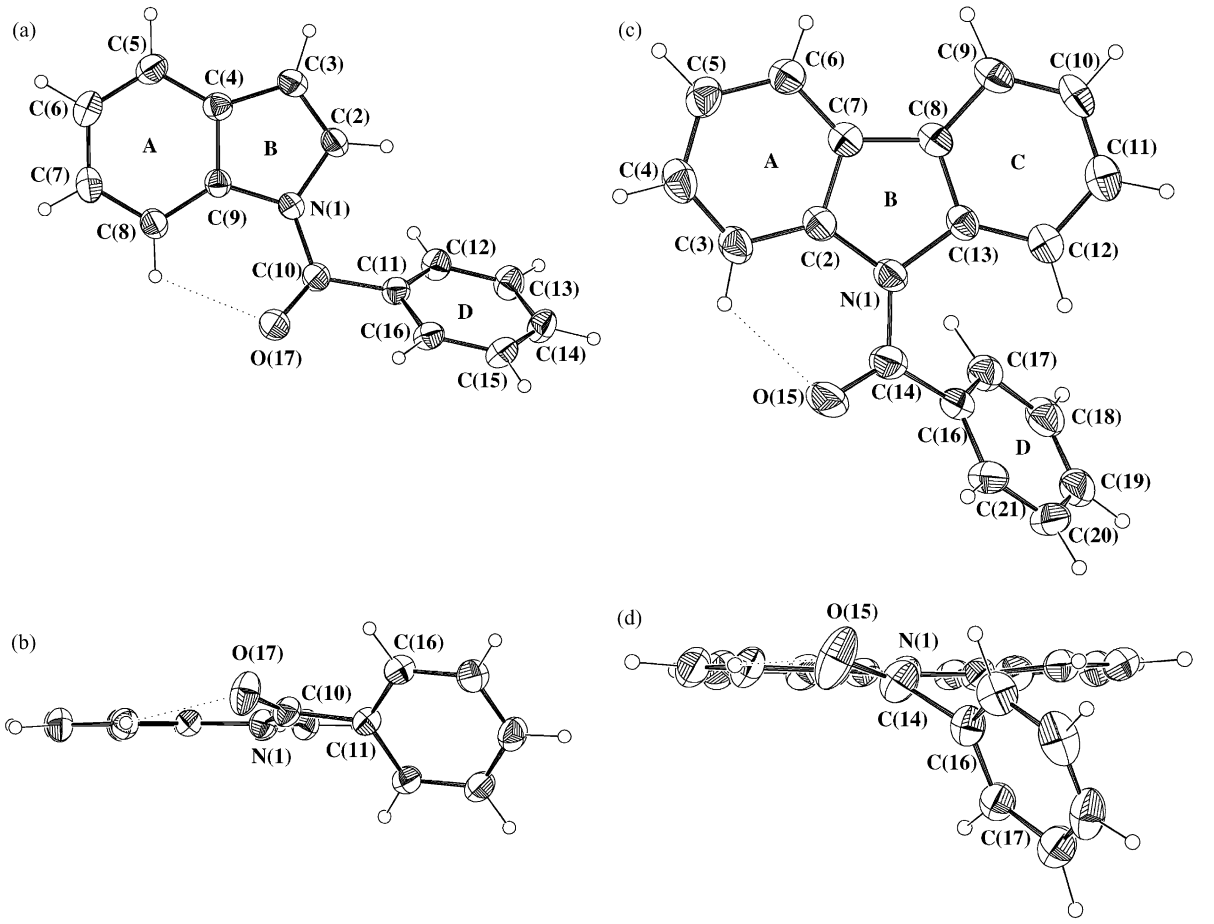

Fig. 1. Two perpendicular views of the molecular structure of compound **3** [(a), (b)] and compound **5** [(c), (d)] showing the numbering scheme and the conformation of the molecules. Thermal ellipsoids are drawn at 30% probability level.

of the six-membered (A or C carbocycles) and the five-membered (B heterocycle) rings, seem to be influenced by the intramolecular C—H···O=C contact as reflected by the C—N—C=O torsion angle, in both compounds, and by the narrowing of the corresponding external angle at N1 mainly in **5** (C2—N1—C14 < C13—N1—C14, Table 1) where the angle between B and C is significantly greater than the A, B one [5.2(2) vs 1.3(2)°]. In addition, the O and C atoms of the carbonyl group deviate from the pyrrole plane by 0.535(2), 0.213(2) in **3** and 0.222(5), −0.127(6) Å in **5**, respectively [see Fig.1(b) and (d)]. The phenyl ring of the substituent has similar dihedral angles in both compounds (Table 1).

The crystal packing of **3** can be described as strands in a head-to-tail arrangement along the **b** axis stabilised by C—H···π contacts [Fig. 2(a)] without other contacts between chains than those of the van der Waals ones. In **5**, C—H···O interactions link molecules into chains along the **c** axis that are then connected by C—H···π contacts [Fig. 2(b)]. The relevance of these hydrogen interactions in the crystal structure of organic molecules as well as in biological molecules is well known as stated by Desiraju and Steiner [19].

2.3. Solution NMR results

We have collected in Tables 2 (^{1}H), 3 (^{13}C) and 4

(^{15}N) the results obtained for compounds **1**–**5**.

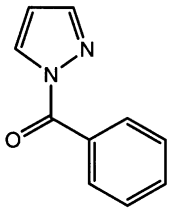

2a

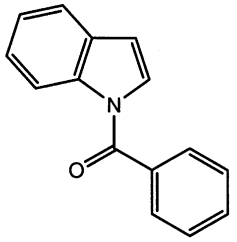

3a

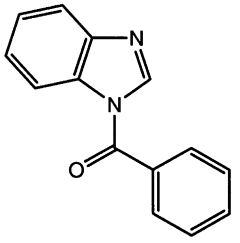

4a

Before discussing these data, we will summarise the previous knowledge on the dynamic aspects of compounds **2**, **3** and **4**. This information, gathered in a recent review [9], come from low temperature NMR experiments. At low temperatures, nothing is observed for pyrazole **2**, indole **3** and benzimidazole **4** derivatives, not necessarily because the barrier should be very low, but because only one conformer is present in solution. These conformers, **2a**, **3a** (see X-ray structure) and **4a** are those predicted from all the previous information gathered on azolides [9].

Therefore, the only compounds where some splitting or, at least broadening, could be expected are **1** (similar populations) and **5** (identical populations of two degenerate rotamers). From data on the barriers of *N*-formyl and *N*-acetylimidazole [9], as well as those on formamides, acetamides and benzamides [22], the estimated barrier for **1** should lie between 30 and 33 kJ mol^{-1}, too low to be determined at 175 K (no broadening observed neither in proton, Table 2, nor in carbon NMR, Table 3).

The barrier of **5** (29.7 kJ mol^{-1}) has been determined by Lunazzi et al. by ^{13}C NMR spectroscopy at 25.16 MHz, but the chemical shifts at 136 K were not reported [20]. Recently, at our request, Professor Lunazzi recorded again the ^{1}H (300.08 MHz) and ^{13}C (75.45 MHz) NMR spectra of **5** in dimethyl ether to which a little acetone-d_6 was added for providing a deuterium lock. The experiments were run at −88°C (185 K, where the rotation is still fast) and at −143°C (130 K) where the rotation process is slow. The ^{1}H NMR spectrum at −143°C is shown in Fig. 3.

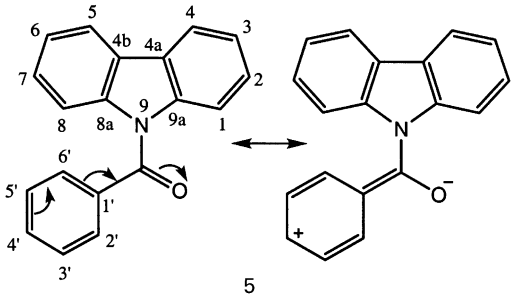

5

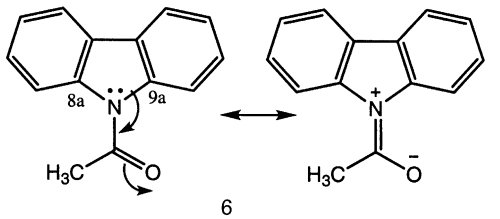

6

The ^{13}C spectrum at 130 K shows a splitting of only 0.4 ppm for carbons C1 and C8 while for 9-acetylcarbazole (**6**), the observed splitting is much larger (3.0 ppm) [20]. It is interesting to compare the four compounds of Scheme 1 (NMR data of **6** and **7** from Ref. [9]).

All the chemical shifts are quite consistent. The fact that on going from **7** to **3**, H(7) moves from 8.37 to 8.59 while from **6** to **5** the shift is opposite in sign (8.60–8.52 ppm) may be related to the twisted structure of **5** and the probable non existence of the weak hydrogen bond between H(1) and the C=O, present in **3** and probably in **6** and **7**. The main difference between the acetyl and the benzoyl series concerns the region opposite to the oxygen where the effect of the phenyl

Table 2
^{1}H Chemical shifts (ppm from TMS) and some ^{1}H–^{1}H coupling constants of *N*-benzoylazoles **1**–**5** at different temperatures

Comp.	Solv. (T, K)	H(2)	H(3)	H(4)	H(5)	H(6)	H(7)	H(2′)	H(3′)	H(4′)
1	$CDCl_3$ (303)	8.05	–	7.13	7.51	–	–	7.76	7.53	7.65
1	C_6D_6 (303)	7.80	–	7.01	7.22	–	–	7.28	6.92	7.06
1	DMSO-d_6 (303)	8.18	–	7.16	7.66	–	–	7.82	7.60	7.73
1	THF-d_8 (303)	8.05	–	7.07	7.58	–	–	7.83	7.57	7.68
1	THF-d_8 (175)	8.34	–	7.24	7.91	–	–	7.96	7.69	7.80
2	$CDCl_3$ (300)	–	7.80	6.52	8.43	–	–	8.12	7.50	7.60
2	THF-d_8 (300)	–	7.79	6.56	8.50	–	–	8.20	7.48	7.60
			$J_{34} = 1.5$	$J_{45} = 2.8$	$J_{35} = 0.7$					
2	THF-d_8 (175)	–	7.99	6.76	8.25	–	–	8.13	7.59	7.71
3	$CDCl_3$ (303)	7.31	6.62	7.62	7.33	7.40	8.42	7.75	7.53	7.61
3	THF-d_8 (303)	7.37	6.64	7.60	7.27	7.34	8.43	7.75	7.53	7.61
3	THF-d_8 (173)	7.62	6.83	7.73	7.39	7.46	8.59	7.88	7.66	7.74
4	$CDCl_3$ (303)	8.22	–	7.84	7.42	7.46	8.19	7.80	7.59	7.69
4	THF-d_8 (303)	8.31	–	7.77	7.38	7.41	8.21	7.88	7.60	7.69
4	THF-d_8 (170)	8.69	–	7.89	7.50	7.54	8.34	8.02	7.72	7.81
		H(1)	H(2)	H(3)	H(4)	–	–	H(2′)	H(3′)	H(4′)
		H(8)	H(7)	H(6)	H(5)			H(6′)	H(5′)	
5	$CDCl_3$ (303)	7.52	7.32	7.36	8.01	–	–	7.73	7.53	7.65
5	THF-d_8 (303)	7.48	7.27	7.31	8.06	–	–	7.70	7.53	7.65
5	CH_3OCH_3 (185)[a]	7.48 (vb)	7.30	7.36	8.13			7.72	7.55	7.69
5	CH_3OCH_3 (130)[a]	8.524	7.60[b]	7.482	8.236			7.767	7.599	7.740
		6.464	7.156	7.319	8.236					
Center		7.494	7.378	7.400	8.236					
Splittings		2.06	0.44	0.08	0.00					

[a] Professor Lunazzi measurements (vb: very broad).
[b] Under the 7.599 signal.

group on the adjacent protons is deshielding in **3** and shielding in **5**.

The assignments of the signals (^{1}H, Table 2 and ^{13}C, Table 3) of compound **5** at 303 K in $CDCl_3$ has been done using the following techniques: (i) directly linked protons and carbons are detected by direct C,H correlation (HMQC); (ii) in $CDCl_3$ long distance correlation shows that C(1) (115.8 ppm) and H(2′,6′)

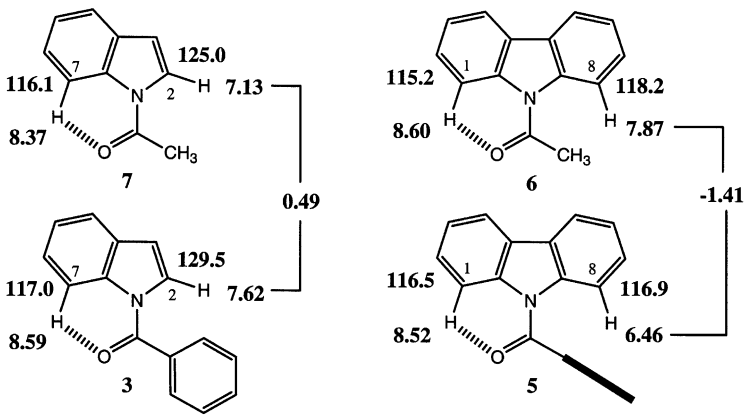

Scheme 1.

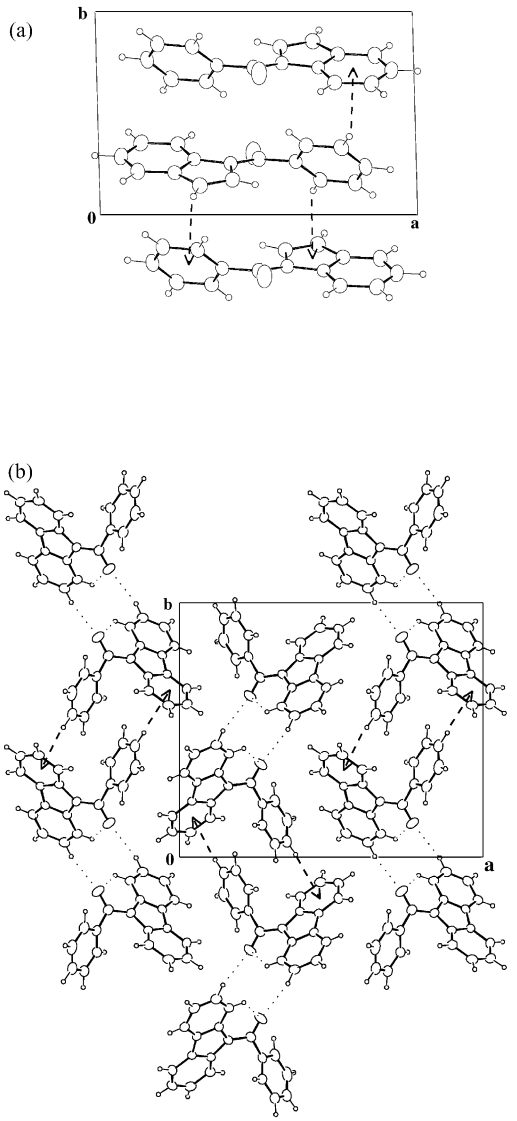

Fig. 2. Crystal packing along the **c** axis: (a) compound **3** and (b) compound **5**. Dotted and dashed lines represent C—H···O hydrogen interactions and C—H···π contacts, respectively.

(7.73 ppm) are close and a NOE2D experiment proves the proximity of H(1) (7.52 ppm) and H(2′,6′) (7.73 ppm). These experiments are still clearer in THF-d_8 where the proton spectrum is better resolved.

Since the data on ^{15}N chemical shifts and ^{1}H–^{15}N coupling constants of azolides are scarce, we have collected in Table 4 those of compounds **1**–**5**.

2.4. Solid state NMR (^{13}C CPMAS)

The ^{13}C CPMAS NMR spectrum of 1-benzoylindole (**3**) is virtually identical to that obtained in solution [see Table 3 and Fig. 4(a)] proving that the structure should be very similar in both phases. On the other hand, the spectrum of 9-benzoylcarbazole (**5**) is much more complex in the solid state than in solution [see Fig. 4(b)]. Part of the complexity arises from the absence of free rotation about the N(9)—C=O and O=C—C(1′) bonds which splits all the signals of the carbazole ring and most of those of the phenyl ring, but the complexity is such that it cannot be due only to this fact.

We have assumed that in the CPMAS spectrum [Fig. 4(b) and Table 3] there is a double splitting: the first is similar to the one observed in solution at 130 K for the carbazole signals C(1) to C(9a); the second one is another expected splitting affecting carbon atoms C(2′)/C(6′) and C(3′)/C(5′) because the barrier about O=C—C(1′) is too low to be slowed in solution while in the solid state these carbons are structurally different. Due to a lack of resolution, in a previous publication, reporting results at 50 MHz, we were unable to observe splitted signals in the case of 9-acetylcarbazole (**6**) [6], although they have been observed in solution at 25 MHz [20].

However, the most extraordinary feature of the ^{13}C CPMAS spectrum of compound **5** is the presence of a second splitting [see Fig. 4(b): CPMAS spectrum] which affects the C=O group and several other carbon atoms. The only possible explanation is the presence in the crystal of two different molecules of **5**. This is apparently in contradiction with the crystallographic result that there is only one independent molecule. Note, however, that compound **5** exists in the studied crystal as a single enantiomer. The other enantiomer [by rotation about the two bonds of the N(9)—CO—C(1′) moiety] is certainly present in the crystallisation crop. This spontaneous resolution indicates that the crude product is a conglomerate and not a racemate [21]. Therefore, we make the following suggestion: *the second splitting is due to the conglomerate structure*. We propose that before the two enantiomers were separated by crystallisation, the conglomerate contained them in different conformations, which are responsible for the second splitting. The values, in ppm, of the second one are also

Table 3
^{13}C Chemical shifts (ppm from TMS) and some $^{1}H-^{13}C$ coupling constants of *N*-benzoylazoles **1–4** at different temperatures

Comp.	Solv. (T, K)	C(2)	C(3)	C(4)	C(5)	C(6)	C(7)	C(3a)	C(7a)	CO	C_6H_5
1	$CDCl_3$ (303)	138.1	–	130.8	117.9	–	–	–	–	166.8	131.8 C(1′) 129.6 C(2′,6′) 128.8 C(3′,5′) 133.5 C(4′)
1	C_6D_6 (303)	138.3	–	131.3	117.9	–	–	–	–	165.9	132.4 C(1′) 129.7 C(2′,6′) 128.7 C(3′,5′) 132.9 C(4′)
1	DMSO-d_6 (303)	138.4	–	130.4	118.4	–	–	–	–	166.1	131.7 C(1′) 129.8 C(2′,6′) 128.9 C(3′,5′) 133.5 C(4′)
1	THF-d_8 (303)	139.0 $^{1}J = 215.2$	–	131.5 $^{1}J = 190.5$	118.7 $^{1}J = 195.7$	–	–	–	–	166.7	133.5 C(1′) 130.7 C(2′,6′) 129.6 C(3′,5′) 134.0 C(4′)
1	THF-d_8 (175)	140.0	–	131.4	118.8	–	–	–	–	167.0	133.1 C(1′) 131.3 C(2′,6′) 129.8 C(3′,5′) 134.4 C(4′)
2	THF-d_8 (300)	–	144.9	109.9	131.0	–	–	–	–	166.4	132.7 C(1′) 132.7 C(2′,6′) 128.6 C(3′,5′) 133.6 C(4′)
2	THF-d_8 (175)	–	145.7	110.8	131.4	–	–	–	–	166.7	132.3 C(1′) 132.8 C(2′,6′) 128.8 C(3′,5′) 134.0 C(4′)
3	$CDCl_3$ (303)	127.5 $^{1}J = 189.7$	108.7 $^{1}J = 175.1$	120.8 $^{1}J = 160.1$	123.8 $^{1}J = 159.4$	124.8 $^{1}J = 160.1$	116.7 $^{1}J = 168.0$	130.3	135.9	168.5	134.5 C(1′) 129.0 C(2′,6′) 128.4 C(3′,5′) 131.7 C(4′)
3	THF-d_8 (303)	128.6	108.7	121.5	124.4	125.6	117.1	131.8	137.1	168.9	135.9 C(1′) 130.0 C(2′,6′) 129.3 C(3′,5′) 132.5 C(4′)
3	THF-d_8 (173)	129.5	108.7	121.8	124.7	125.5	117.0	131.7	136.7	169.2	135.3 C(1′) 130.6 C(2′,6′) 129.5 C(3′,5′) 133.0 C(4′)
3	CPMAS	126.4	107.4	119.5	122.7	122.7	116.7	130.4	135.7	168.6	134.8 C(1′) 128.8 C(2′,6′) 128.8 C(3′,5′) 132.0 C(4′)
4	$CDCl_3$ (303)	143.0	–	120.6	125.3	125.8	115.4	144.0	132.1	167.1	132.9 C(1′) 129.5 C(2′,6′) 129.0 C(3′,5′) 133.2 C(4′)
4	THF-d_8 (303)	144.4 $^{1}J = 215.0$	–	121.2 $^{1}J = 162.9$	125.5 $^{1}J = 159.9$	125.9 $^{1}J = 160.5$	116.1 $^{1}J = 167.4$	145.7	133.5	167.1	134.5 C(1′) 130.5 C(2′,6′) 129.6 C(3′,5′) 133.5 C(4′)

Table 3 (*continued*)

Comp.	Solv. (T, K)	C(2)	C(3)	C(4)	C(5)	C(6)	C(7)	C(3a)	C(7a)	CO	C_6H_5
4	THF-d_8 (170)	145.8	–	121.0	125.8	126.1	116.2	145.2	133.1	168.2	134.1 C(1′) 131.2 C(2′,6′) 129.8 C(3′,5′) 133.9 C(4′)
						Carbazole					
		C(1) C(8)	C(2) C(7)	C(3) C(6)	C(4) C(5)	C(4a) C(4b)	C(8a) C(9a)	C=O C(2′,6′)	C(1′) C(3′,5′)		C(4′)
5	$CDCl_3$ (303)[a]	115.8	126.7	123.4	119.8	126.0	139.2	169.6	135.8		
		115.8	126.7	123.4	119.8	126.0	139.2	129.0	128.9	132.3	
5	MeOMe (185)[b]	116.69	127.64	124.29	120.99	126.82	140.12	170.03	137.06		
		116.69	127.64	124.29	120.99	126.82	140.12	130.19	129.93	133.44	
5	MeOMe (130)[b]	116.56	127.06	123.99	121.39	126.72	140.36	170.11	136.93		
		116.94	128.46	124.84	121.08	126.66	139.45	130.31	130.00	133.58	
	Splittings	C(1,8)	C(2,7)	C(3,6)	C(4,5)	C(4a,4b)	C(8a,9a)				
		0.38	1.40	0.85	0.31	0.06	0.91				
	CPMAS[a]	114.8	125.6	124.0	120.4	124.8	138.8	167.3	135.8		
		113.8			118.7		138.3	166.2	135.4		
		115.7			122.1		139.3	168.4	136.2		
		115.7	126.9	124.8	119.4	124.8	137.9	130.7	128.8	131.8	
		114.8			118.2		137.5	129.7	128.0	131.2	
		116.6			120.7		138.3			132.4	
	Splittings	0.9	1.3	0.8	1.0	0.0	0.9				
		1.9			3.4		1.0	2.2	0.8	1.2	
		1.8			2.5		0.8		0.8		

[a] This work.
[b] Professor Lunazzi measurements.

reported in Table 3 (probably there are other small splittings). According to these values, the largest perturbation due to the conglomerate arises in the proximity of the C(4)/C(5) part of the molecule.

3. Theoretical calculations

3.1. Geometries

The comparison between the geometries of 9-acetyl **6** [10] and 9-benzoylcarbazole **5** (this work) concerning the "amide" fragment show the following features (from **6** to **5**): (i) concerning the N—C and C=O, distances, the first one shows a lengthening of 0.005 Å and the second one a shortening of 0.002 Å; (ii) about the N—C=O and N—C—C angles, the first one increases (0.27 Å) and the second one decreases (1.16 Å). These features are probably related to differences in the resonance forms (see formulae **5** and **6**).

The most significant difference between both azolides concerns the dihedral angle θ[C(9a)—N(9)—C=O]. While **6** is planar ($\theta = 0.00°$), **5** is twisted ($\theta = -37.2°$). This fact has probably more influence, on the lowering of the barrier to the rotation, than the lengthening of the N—C bond. In compound **6**, C(1) is rather close to the oxygen [a C(19)—H···O=C weak hydrogen bond is reasonable] and C(8) to the methyl group; to this situation corresponds a difference of

Table 4
Chemical shifts (ppm from nitromethane for ^{15}N) and some $^{1}H-^{15}N$ coupling constants (Hz) (the coupling constants have been measured on the $^{1}H-^{15}N$ 2D spectra) of *N*-benzoylazoles at room temperature (~300 K)

Comp.	Solvent	N(1)	N(2)	N(3)
1	THF-d_8	− 176.3 $^{2}J = 7$, H(2)	–	− 110.3 $^{2}J = 11$, H(2) $^{2}J = 7$, H(4)
1	DMSO-d_6	− 174.6 $^{2}J = 7$, H(2)	–	− 109.6 $^{2}J = 12$, H(2) $^{2}J = 7$, H(4)
2	THF-d_8	− 143.0	− 71.2	–
3	$CDCl_3$	− 204.4 $^{2}J = 8$, H(2) $^{3}J = 7$, H(3)	–	–
4	THF-d_8	− 192.9 $^{2}J = 9$, H(2)	–	− 123.3 $^{2}J = 12$, H(2)
5	$CDCl_3$	− 218.6 [N(9)]	–	–

3.0 ppm. In compound (**5**) the non-planar conformation lowers this difference to 0.4 ppm.

Finally, there are some differences between the experimental and calculated geometries for compound **5**: N—C 1.400/1.394 Å, C=O 1.212/1.187 Å, N—C=O 119.3/121.0° and θ −23.5/−37.2°, but they are small enough to consider that the calculated molecule is a good approximation to the solid state one.

3.2. Absolute shieldings

For compound **5** we have used the same basis set (RHF/6-311G**) as in our previous work on *N*-acetylazoles for the sake of consistency [10]. The absolute shieldings, in ppm, were calculated within the GIAO approximation (see experimental part) and are: C(1) 76.20, C(2) 63.21, C(3) 69.06, C(4)

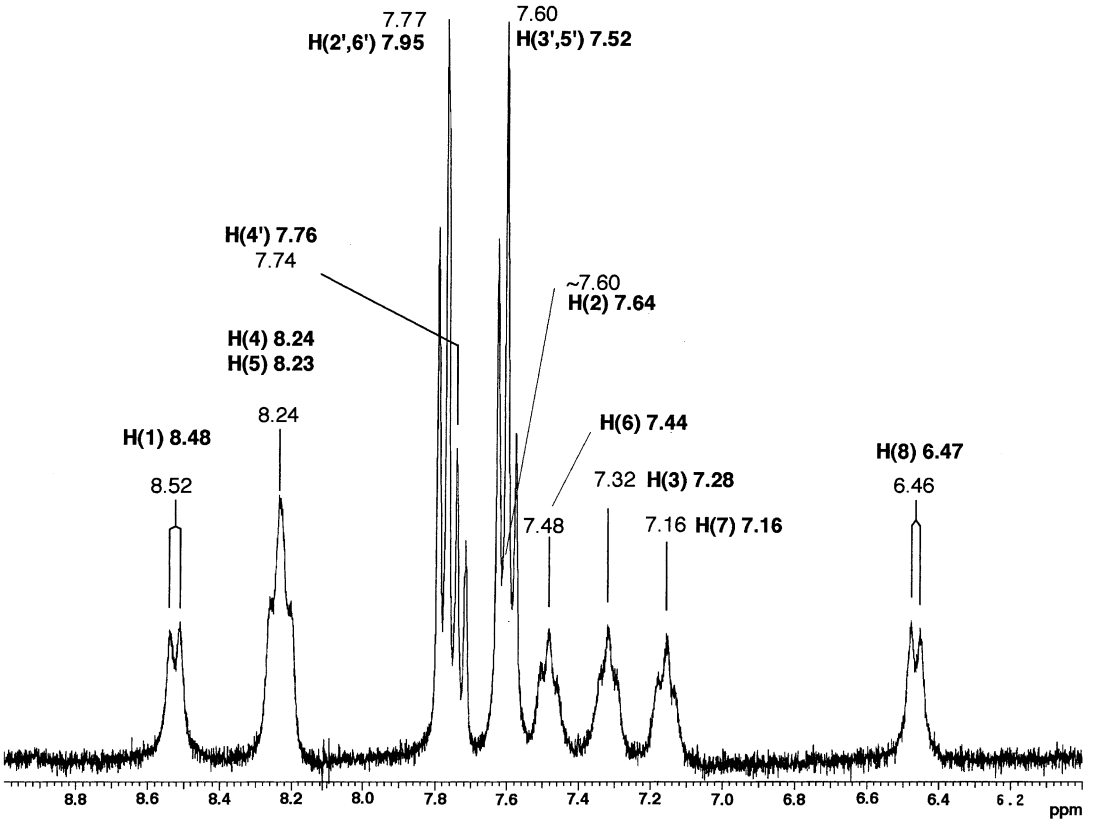

Fig. 3. Experimental ^{1}H NMR spectrum of **5** at −138°C and 300.08 MHz (in bold, the values of the model and the assignment).

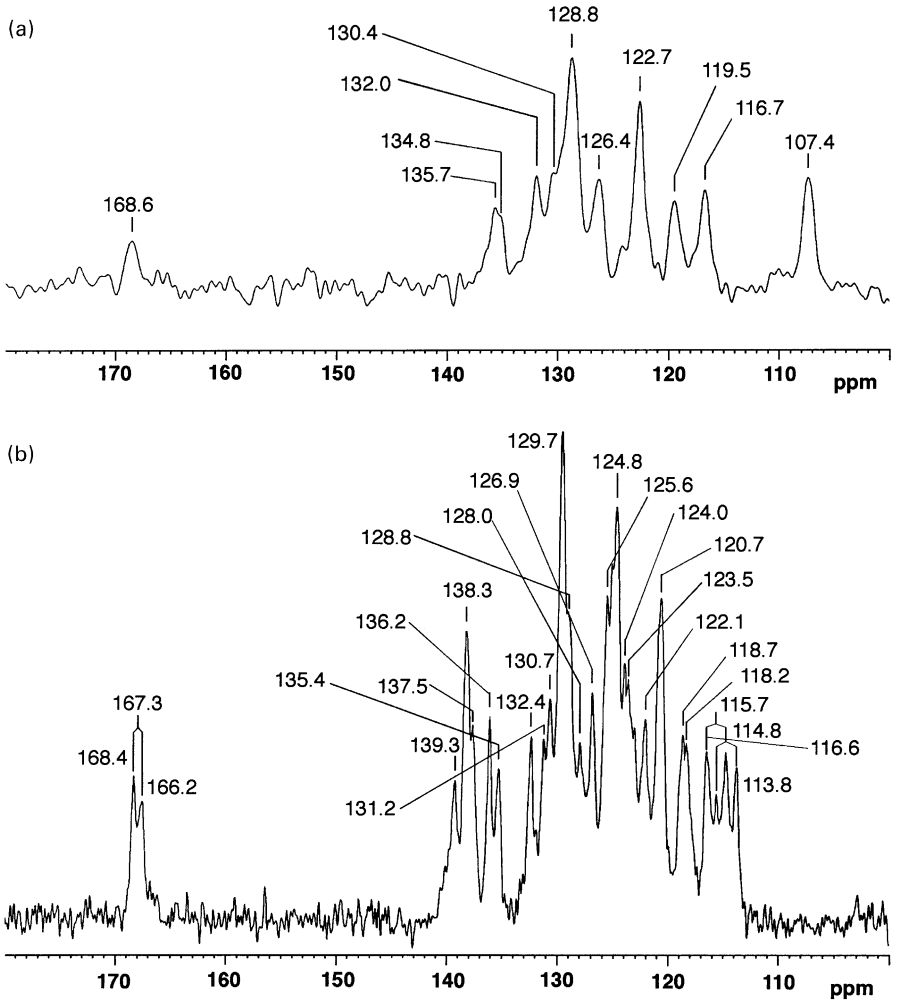

Fig. 4. (a) Experimental ^{13}C CPMAS spectrum of **3** at 125 MHz. (b) Experimental ^{13}C CPMAS spectrum of **5** at 125 MHz.

68.13, C(4a) 65.11, C(4b) 66.39, C(5) 69.20, C(6) 68.23, C(7) 61.33, C(8) 74.38, C(8a) 48.28, N(9) 110.80, C(9a) 49.72, C(O) 22.66, (O) -153.55, C(1′) 54.83, C(2′) 56.73, C(3′) 62.13, C(4′) 56.04, C(5′) 63.68, C(6′) 57.96, H(1) 23.72, H(2) 24.59, H(3) 24.80, H(4) 23.97, H(5) 23.98, H(6) 24.96, H(7) 25.08, H(8) 25.80, H(2′) 23.81, H(3′) 24.53, H(4′) 24.47, H(5′) 24.89 and H(6′) 24.73.

For ^{13}C NMR, we have compared the experimental chemical shifts at 130 K (Table 3) as well as the CPMAS data (centre of the multiplet) with the absolute shieldings corrected by 204.3 ppm to account for the reference. The C=O signal was excluded:

$$\delta^{13}\text{C solution} = (0.905 \pm 0.002)[204.3 - \sigma^{13}C \text{ calculated}], \quad (1)$$

$$n = 22,\ r^2 = 1.000$$

$$\delta^{13}\text{C CPMAS} = (0.896 \pm 0.002)[204.3 - \sigma^{13}C \text{ calculated}], \quad (2)$$

$$n = 18,\ r^2 = 1.000$$

These equations predict for the C=O, 164.4 instead of 170.1 (solution) and 162.7 instead of 167.3 ppm (solid). At this level of calculations, aromatic and C=O carbons are mutually inconsistent.

The ^{1}H NMR spectrum is in good agreement with the calculated shieldings, in this case all H atoms are linked to aromatic carbons (32.47 is the absolute shielding of TMS):

$$\delta^1\text{H solution} = (0.969 \pm 0.002)[32.47 - \sigma^1\text{H calculated}], \quad (3)$$

$$n = 15,\ r^2 = 1.000$$

The largest difference (see Fig. 3) is found for the H(2′,6′) protons. This is probably related to the conformation of the benzoyl group about the C(1′)—CO bond. The calculations correspond to a fixed conformation and the experimental value to free rotation (although with different populations of the rotamers). According to the calculations, the proton H(2′) close to the C=O and the proton C(6′) close to H(8) should appear at 8.39 and 7.50 ppm, respectively, in the twisted conformation.

In our previous paper about azolides, we have described an empirical relationship between the absolute shieldings (calculated at the same level) and the chemical shifts for the ^{15}N nucleus ($\delta^{15}\text{N} = -130 - 0.75\sigma^{15}\text{N}$) [10]. In the case of **5**, $\sigma^{15}\text{N}(9) = 110.80$ ppm which corresponds to $\delta^{15}\text{N} = -212.5$ ppm, close to the experimental value of −218.6 (Table 4).

4. Conclusions

The combined use of crystallography, CPMAS NMR, low temperature solution NMR and ab initio calculations (including absolute shieldings) is an extraordinarily powerful tool to understand the solid state and its relation with solution. Thanks to this approach, the assignment of all the signals of compound **5** in solution at low temperature has been possible. This compound presents a case of spontaneous resolution, although in solution both enantiomers equilibrate very quickly due to its low activation barrier (about 30 kJ mol^{-1}). Most structural work on azolides has been done on *N*-acetyl derivatives [9], the present work extends these studies to the almost unexplored field of *N*-benzoylazoles.

5. Experimental

5.1. Materials

Melting points were determined with a hot-stage microscope and are uncorrected. IR spectra were recorded in a Philips PU9714. Column chromatography was performed on silicagel Merck 60 (70–230 mesh) using the appropriate eluent.

Compounds **1** to **5** have been prepared according to one of the two following procedures, depending on the acidity of the NH. For azolides **1**, **2** and **4** procedure 1 has been used. The azole (25.5 mmol) in solution in a dry solvent (50 mL) was placed in a three-necked, round bottomed flask provided with a condenser under argon atmosphere and with magnetic stirring. To this solution 1.5 mL (12.75 mmol) of benzoyl chloride (99%, d = 1.21 g cm^{-3}) were added and the mixture was maintained at r.t. for 24 h. The solution was filtered off (azole hydrochloride) under argon and the solvent evaporated; an oil remains. 1-Benzoylimidazole **1**, solvent benzene, oil, yield 94%. 1-Benzoylpyrazole **2**, solvent diethyl ether, m.p. 47–48°C, yield 75%. 1-Benzoyl-benzimidazole **4**, solvent tetrahydrofuran, m.p. 93.0–93.5°C, yield 86%, IR (KBr cm^{-1}) $\nu_{C=O} = 1665$. For azolides **3** and **5** procedure 2 has been used. A solution of azole (30 mmol) in 150 mL of a mixture of dry benzene/dimethylformamide (1:1 ratio) was placed in an ice/salt bath. To this solution 60% NaH (1.2 g, 30 mmol) was added and the reaction mixture magnetically stirred for 30 min. After cooling, 4.21 g (30 mmol) of benzoyl chloride (99%, d = 1.21 g cm^{-3}) in 10 mL of benzene were added controlling that the temperature remains below 0°C, then the mixture was left at r.t. for 2 h. Sodium chloride was filtered off and the solution evaporated under vacuum. After column chromatography using hexane:EtOAc 9:1, azolides **3** and **5** were obtained. 1-Benzoylindole **3**, m.p. 68.0–68.5°C, 60% yield, IR (KBr cm^{-1}) $\nu_{C=O} = 1665$. 9-Benzoylcarbazole **5**, m.p. 98–100°C, 63% yield, IR (cm^{-1}) $\nu_{C=O} = 1665$.

Table 5
Crystal analysis parameters at room temperature

	3	**5**
Crystal data		
Chemical formula	$C_{15}H_{11}NO$	$C_{19}H_{13}NO$
Crystal colour	Colourless	Colourless
Crystal description	Prism	Prism
Crystal size (mm)	$0.67 \times 0.50 \times 0.50$	$0.40 \times 0.13 \times 0.13$
Crystal system	Triclinic	Orthorhombic
Mr	221.258	271.318
Space group	$P\bar{1}$	$P2_12_12_1$
a/Å	12.1874(7)	17.2138(20)
b/Å	7.6925(4)	14.4042(16)
c/Å)	6.2297(3)	5.5668(7)
α/°	97.226(5)	90
β/°	101.756(4)	90
γ/°	90.047(7)	90
Z	2	4
Dx/gr cm^{-3}	1.296	1.306
V/Å^3	567.04(5)	1380.3(3)
No. reflections for lattice parameters:	67	43
θ range for lattice parameters:	2–45(°)	2–45(°)
Absorption coefficient (cm^{-1})	6.46	6.36
Data collection		
Diffractometer type	Philips PW1100	Seifert XRD3000-S
	Graphite oriented monocromator.	
	Measurement time: 1 min./reflection.	
	Detector apertures: 1×1 (°)	
	Collection method: w/2θ scans,	
	Scan width = 1.6 (°)	
	Two standard reflections every 100 min:	
	No variation	
θmax(°)	67.0	67.5
No. of independent reflections	2022	1292
No. of observed reflections	1908($I > 2\sigma(I)$ criterion)	909($I > 1\sigma(I)$ criterion)
Refinement		
Treatment of hydrogen atoms	Difference synthesis	
Refinement	Least-squares on Fo, Full matrix	
R, wR	0.040, 0.061	0.051, 0.059
No. of parameters refined	199	243
Extinction parameters ($\times 10^{-4}$)	0.44(6)	0.07(1)
Degrees of freedom	1709	666
Ratio of freedom	9.6	3.7
($\Delta\rho$)max (e/Å^3)	0.21	0.23
⟨Shift/error⟩	0.001	0.011
Max. thermal value (Å^2)	U22[O17] = 0.131(2)	U33(O15) = 0.168(6)

5.2. NMR spectroscopy

The ^{1}H and ^{13}C and ^{15}N NMR spectra in solution were recorded on a Bruker DRX-400 instrument working at 400.13 (^{1}H), 100.62 (^{13}C) and 40.56 MHz (^{15}N) using standard conditions. Solid state ^{13}C CPMAS NMR spectra were recorded at 300 K using a Bruker DSX 500 instrument (125.77 MHz) with a 4 mm probe, a 10 kHz rotation frequency and standard CP pulse sequences were employed. Chemical shifts (δ) in ppm are referred to external Me_4Si for ^{1}H and ^{13}C and to external NO_2CH_3 for ^{15}N NMR spectra.

5.3. X-ray crystallography

Crystal data and experimental details are given in Table 5. The structures were solved by direct methods (SIR97) [23]. The lack of suitable anomalous scatters in compound **5** did not allow us to determine the absolute configuration of the conformational enantiomer studied as illustrated by the value of −0.3(17) obtained for the Flack parameter [24] and thus the Friedel pairs were merged. The weighting schemes were established [25] in an empirical way as to give no trends in $\langle w\Delta^2 F\rangle$ vs $\langle \mathrm{Fo}\rangle$ or $\langle \sin\theta/\lambda\rangle$: $w = K/[(a + b\cdot \mathrm{Fo})^2][c + d\cdot \sin\theta/\lambda]$; the a, b, c and d parameters were adjusted to flatten the initial trends. Secondary extinction correction was applied (Table 5) according to the Zachariasen formalism [26]. The scattering factors were taken from the International Tables for X-Ray Crystallography [27]. Most of the calculations were performed using the Xtal3.6 system of programs [28].

The CIF files were deposited with the Cambridge Crystallographic Data Center (CCDC 149366 and 149367).

5.4. Computational details

Geometry optimisation on compound **5** was carried out at the RHF/6-311G** level of the theory [29,30] and absolute shielding calculated over that geometry within the GIAO approximation [31,32]. All these calculations were carried out using the Gaussian 98 facilities [33].

Acknowledgements

Financial support was provided by the Spanish DGICYT (Project nos. BQU-2000-0252 and BQU-2000-0868) and by the Comunidad de Madrid (07N/0001/1999). We thank Dr. Stefan Steuernagel (Bruker Spectrospin GmbH) for recording the ^{13}C CPMAS spectra of compounds **3** and **5** with a DSX 500 MHz instrument. This work would have been completely different if Professor Ludovico Lunazzi (University of Bologna) would have not studied the NMR spectroscopy of compound **5** at very low temperatures: our most warmest thanks.

References

[1] J. Elguero, A. Fruchier, R. Jacquier, Bull. Soc. Chim. Fr. (1966) 3041.
[2] L. Pappalardo, J. Elguero, C. Marzin, C.R. Acad. Sci. Ser. C 277 (1973) 1163.
[3] J. Elguero, C. Marzin, L. Pappalardo, Bull. Soc. Chim. Fr. (1974) 1137.
[4] J. Elguero, C. Marzin, M.E. Peek, Org. Magn. Reson. 7 (1975) 445.
[5] M. Begtrup, R.M. Claramunt, J. Elguero, J. Chem. Soc. Perkin Trans. 2 (1978) 99.
[6] R. Faure, E.J. Vincent, A. Rousseau, J. Elguero, Heterocycles 26 (1987) 333.
[7] A. Maquestiau, Y. van Haverbeke, R. Flammang, R.M. Claramunt, J. Elguero, Bull. Soc. Chim. Fr. (1975) 2693.
[8] A. Maquestiau, A. Tommasetti, C. Pedregal, J. Elguero, R. Flammang, Bull. Soc. Chim. Belg. 93 (1984) 1057.
[9] J. Elguero, C. Foces-Foces, D. Sanz, R.M. Claramunt, Azolides: Structural aspects, in: C.J. Moody (Ed.), Advances in Nitrogen Heterocycles, vol. IV, Jay Press Inc, Stamford, Conneticut, 2000, pp. 295–367.
[10] R.M. Claramunt, D. Sanz, I. Alkorta, J. Elguero, C. Foces-Foces, A.L. Llamas-Saiz, J. Heterocycl. Chem. 38 (2001) 443.
[11] H.A. Staab, Angew. Chem. Int. Ed. 1 (1962) 351.
[12] W. Hückel, H. Bretschneider, Ber. Dtsch. Chem. Ges. 70 (1937) 2024.
[13] P. Grammaticakis, C. R. Hebd. Seances Acad. Sci. 250 (1960) 4373.
[14] T.H. Fife, R. Natarajan, M.H. Werner, J. Org. Chem. 52 (1987) 740.
[15] Y.H.R. Jois, H.W. Gibson, J. Org. Chem. 56 (1991) 865.
[16] S. Ghosh, D.B. Datta, I. Data, T.K. Das, Tetrahedron 45 (1989) 3775.
[17] F.H. Allen, J.E. Davies, J.J. Galloy, O. Johnson, O. Kennard, C.F. Macrae, E.M. Mitchell, J.F. Mitchell, J.M. Smith, D.G. Watson, J. Chem. Info. Comput. Sci. 31 (1991) 187.
[18] T. Kaneko, M. Matsuo, Y. Iitaka, Chem. Pharm. Bull. 29 (1981) 3499.
[19] G.R. Desiraju, T. Steiner, The Weak Hydrogen Bond in Structural Chemistry and Biology, Oxford University Press, Oxford, 1999.
[20] A. Cipiciani, P. Linda, D. Macciantelli, L. Lunazzi, J. Chem. Soc. Perkin Trans. 2 (1979) 1045.
[21] J. Jacques, A. Collet, S.H. Wilen, Enantiomers, Racemates, and Resolutions, Krieger Publishing Co, Malabar, FL, 1994.
[22] W.E. Stewart, T.H. Siddall, Chem. Rev. 70 (1970) 517.
[23] A. Altomare, G. Cascarano, C. Giacovazzo, A. Guagliardi, A.G.G. Moliterni, M.C. Burla, G. Polidori, M. Camalli, R. Spagna, SIR97. A Package for Crystal Structure Solution by Direct methods and Refinement, University of Bari, Italy, 1997.
[24] H.D. Flack, Acta Crystallogr, Sect. A 39 (1983) 876.
[25] M. Martinez-Ripoll, F.H. Cano, 'PESOS' unpublished program, Instituto Rocasolano, CSIC, Spain, 1975.
[26] W.H. Zachariasen, Acta Crystallogr. 23 (1967) 558.
[27] International Tables for X-Ray Crystallography, 1974, Birmingham, Kynoch Press, England.

[28] S.R. Hall, D.J. du Boulay, R. Olthof-Hazekamp (Eds.), The Xtal System of Crystallographic Software, 'Xtal3.6' User's Manual, The University of Western Australia, Australia, 1999.
[29] A.D. McLean, G.S. Chandler, J. Chem. Phys. 72 (1980) 5639.
[30] R. Krishnan, J.S. Binkley, R. Seeger, J.A. Pople, J. Chem. Phys. 72 (1980) 650.
[31] R. Ditchfield, Mol. Phys. 27 (1974) 789.
[32] F. London, J. Phys. Radium 8 (1937) 397.
[33] Gaussian 98 (Revision A.1), M.J. Frisch, G.W. Trucks, H.B. Schlegel, G.E. Scuseria, M.A. Robb, J.R. Cheeseman, V.G. Zakrzewski, J.A. Montgomery, R.E. Stratmann, J.C. Burant, S. Dapprich, J.M. Millam, A.D. Daniels, K.N. Kudin, M.C. Strain, O. Farkas, J. Tomasi, V. Barone, M. Cossi, R. Cammi, B. Mennucci, C. Pomelli, C. Adamo, S. Clifford, J. Ochterski, G.A. Petersson, P.Y. Ayala, Q. Cui, K. Morokuma, D.K. Malick, A.D. Rabuck, K. Raghavachari, J.B. Foresman, J. Cioslowski, J.V. Ortiz, B.B. Stefanov, G. Liu, A. Liashenko, P. Piskorz, I. Komaromi, R. Gomperts, R.L. Martin, D.J. Fox, T. Keith, M.A. Al-Laham, C.Y. Peng, A. Nanayakkara, C. Gonzalez, M. Challacombe, P.M.W. Gill, B.G. Johnson, W. Chen, M.W. Wong, J.L. Andres, M. Head-Gordon, E.S. Replogle, J.A. Pople, Gaussian, Inc., Pittsburgh, PA, 1998.